

Remarks about the interpretation of impulse experiments in shear flows of viscoelastic liquids

A. Narain and D. D. Joseph

Department of Mechanical Engineering and Engineering Mechanics, Michigan Technological University, Houghton (Michigan/USA) and Department of Aerospace Engineering and Mechanics, University of Minnesota, Minneapolis (Minn./USA)

Abstract: The effect of inertia in three popular impulse experiments in shear flows of viscoelastic liquids is considered. Dynamics of the flow is used to evaluate the stress observables such as the shear stress and the first normal stress difference at the walls. In particular we find that for many linear viscoelastic models with slowly fading memory, the difference between experimental observables and a theory based on the assumption of ignorable inertia could be quite substantial.

Key words: Step jump, first normal-stress difference, reflecting shock waves, relaxation function

Introduction

The limiting velocity distribution for start-up of Couette flow between parallel plates is a linear shear. It is common practice to assume that the real motion is close to linear shear long before the stress approaches its asymptotic steady state. When the linear shear is assumed to hold from the initial instant, the evolution of the wall shear stress is determined by material functions, independent of deformation. These material functions are then determined by experimental measurements. We argue that in many cases only special features of the material functions can be determined by this method because in all cases the early time behavior of the motion is incorrectly given by a linear shear. The assumption that the early part of the stress response can be ignored is fallacious when the dynamics shows the presence of a delta function singularity in the wall shear stress at time $t = 0$ and at subsequent discrete times of reflection off bounding walls. This delta function contribution cannot be ignored even if the steady state is achieved rapidly, because typically the shear remembers the past deformation gradient history at least over a length of time comparable to a representative relaxation time of the material. In fact, the early time behavior is crucial in

the determination of the material functions and it can be obtained from experiments only by using a correct theory based on dynamics. When this is done, it is possible to interpret data showing stress overshoot with linear theories based on commonly used constitutive equations and to interpret early oscillations in the observed values of material functions in terms of repeated reflections off bounding walls.

The foregoing critical remarks apply equally to the interpretation of stress relaxation experiments and other experiments involving impulse changes in velocity and displacement.

In this paper, we present the results of analysis of linearized dynamics, particularly to results which give the early time behavior of observables which depend exclusively on the shear relaxation function $G(s)$. We give many new formulas for the observables in standard rheological tests which we think will be used for the determination of the relaxation modulus in viscoelastic fluids.

1. A summary of previous work on step jumps of velocity and displacement

In our earlier work [12, 13, 14], we treated the problems of step increase in velocity and displacement

using a constitutive expression of the type:

$$T = -pI + \mu A_1 + \int_0^\infty \tilde{\mu}(s) G(s) ds \tag{1.1}$$

where

$$\tilde{\mu}(s) \equiv \frac{dG}{ds} \quad \text{and} \quad G: [0, \infty) \rightarrow R^+ = \{x \in R \mid x > 0\}$$

is assumed to be (i) monotonically decreasing, (ii) continuous and piecewise continuously differentiable, (iii) along with G' of $O(e^{-\tilde{\lambda}s})$ as $s \rightarrow \infty$ for some $\tilde{\lambda} > 0$ and hence $\lim_{s \rightarrow \infty} G(s) = \lim_{s \rightarrow \infty} G'(s) = 0$.

Constitutive equations such as (1.1) may be justified in various ways (see Saut and Joseph [17] and Renardy [16]). We considered two singular problems in which the velocity is assumed to be in the form $V = \hat{e}_y v(x, t)$ in the semi-infinite space above a flat plate and

$$\Omega = [x, y, z; 0 < x < \infty, -\infty < y < \infty, -\infty < z < \infty].$$

At $x = 0$, we imagine either a step-jump in velocity or displacement, satisfying

$$\mu \frac{\partial^2 v}{\partial x^2}(x, t) + \int_0^t G(s) \frac{\partial^2 v}{\partial x^2}(x, t-s) ds = \rho \frac{\partial v}{\partial t}(x, t). \tag{1.2}$$

$$v(x, 0) = 0,$$

$$v(x, t) \text{ is bounded as } x, t \rightarrow \infty.$$

And for step-increase in velocity at $x = 0$

$$v(0, t) = H(t - 0). \tag{1.3}$$

For the step increase in displacement of the bottom plate we have

$$v(0, t) = \delta(t). \tag{1.4}$$

1.1 Linearized simple fluids of Boltzmann type ($\mu = 0$)*

The solution of problem (1.2) and (1.3) is given in § 4-6 of [12] as:

$$v(x, t) = f(x, t) H(t - \alpha x)$$

where

$$c = \frac{1}{\alpha} = \sqrt{G(0)/\rho}$$

and $f(x, t)$ is defined in (5.10) of [12]. Here it will suffice to note that (see [12, 5, 15])

*) This class of fluids ($\mu = 0$) alone show an elastic response. The term *viscoelastic* is probably not appropriate for $\mu \neq 0$.

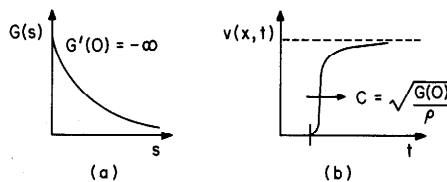


Fig. 1.1. Propagating smooth solutions (b) occur when $G(s)$, satisfying (i), is as sketched in (a). Smooth solutions of this type have been computed by Buchen and Mainardi [3], for a special kernel with the property that $G'(s)$ is proportional to $-s^{-1/2}$ as $s \rightarrow 0$

$$a(x) \stackrel{\text{def}}{=} f(x, \alpha x^+) = \exp(\alpha x G'(0)/2G(0)), \quad \forall x \geq 0,$$

$$\frac{\partial f}{\partial t}(x, \alpha x^+) = -\alpha x \exp\left(\frac{\alpha x G'(0)}{2G(0)}\right) \cdot \left[\frac{3}{8} \left(\frac{G'(0)}{G(0)}\right)^2 - \frac{1}{2} \frac{G''(0)}{G(0)} \right], \quad \forall x \geq 0, \tag{1.5}$$

$$\frac{\partial f}{\partial x}(x, \alpha x^+) = \alpha f(x, \alpha x^+) \cdot \left[\frac{G'(0)}{2G(0)} + \alpha x \left\{ \frac{3}{8} \left(\frac{G'(0)}{G(0)}\right)^2 - \frac{1}{2} \frac{G''(0)}{G(0)} \right\} \right], \quad \forall x \geq 0.$$

If

$$G(s) = k e^{-\mu s},$$

then

$$\frac{3}{8} \left(\frac{G'(0)}{G(0)}\right)^2 - \frac{1}{2} \frac{G''(0)}{G(0)} = -\frac{1}{2} \mu^2 < 0.$$

The solution of step-displacement problem (1.2) and (1.4) is given as (see in (10.7) of [12])

$$v(x, t) = \frac{\partial f}{\partial t}(x, t) H(t - \alpha x) + f(x, \alpha x^+) \delta(t - \alpha x) \tag{1.6}$$

where $f(x, t)$ is the same as in (1.5).

1.2 Special kernels for fluids of the Maxwell type ($\mu = 0$)

There are two special cases ($G'(0) = -\infty, G'(0) = 0$):

- (i) $G'(0) = -\infty$ and $0 < G(0) < \infty$.

In this case the amplitude $a(x)$ of the shock (given in (1.5)) is zero. Thus the discontinuity of the data is removed but the support of the solution propagates with the speed $c = 1/\alpha$.

In fact, Renardy [15] has shown that for a kernel (used in certain molecular models)

$$G'(s) = -\sum_{n=1}^\infty \exp(-n^\alpha s), \quad \alpha > 1,$$

$$G'(0) = -\infty, \quad G(0) = \sum_{n=1}^\infty \frac{1}{n^\alpha},$$

the solution is C^∞ smooth at the support (see Fig. 1.1).

Some form of continuity of solution on kernels possessing nearly identical features globally might be expected. For example, we may construct kernels with $G'(0) = -\infty$ and even with C^∞ contact at the vertical axis whose graphs are indistinguishable from kernels for which $G'(0)$ is finite in all neighborhoods bounded away from $s=0$. This may lead to smooth, shock-like solutions (see Fig. 1.1). Such problems are in some sense like the ones which are perturbed with a small viscosity μ . We shall remark in § 1.3, that the small viscosity leads to a transition layer of size μ which collapses onto a shock as $\mu \rightarrow 0$. For small μ the solution is smooth, but shock-like (see Figs. 1.1, 1.3). The heuristic argument for the equivalence of problems for kernels of type (i) with those perturbed by a small viscosity is as follows. We are given $G(s)$, $s > 0$ such that $G(0)$ is finite, $G'(s) < 0$, $s > 0$, and $G'(0) = -\infty$. Now we implement the construction of a comparison kernel of Maxwell type. First choose a small time ε . Then, at $G(\varepsilon)$ draw the tangent $G'(\varepsilon)$. This tangent pierces $s=0$ at the value $G_M(0)$. Define $G_M(s)$ *)

$$G_M(s) = \begin{cases} G'(\varepsilon)s + G_M(0), & s \leq \varepsilon, \\ G(s), & s > \varepsilon. \end{cases}$$

We may write

$$\begin{aligned} \int_0^t G(s) \frac{\partial^2 v}{\partial x^2}(x, t-s) ds \\ = \int_0^\varepsilon G_M(s) \frac{\partial^2 v}{\partial x^2}(x, t-s) ds \\ + \int_0^\varepsilon (G(s) - G_M(s)) \frac{\partial^2 v}{\partial x^2}(x, t-s) ds. \end{aligned}$$

Using the mean value theorem the last integral may be written as

$$\varepsilon [G(\bar{s}) - G_M(\bar{s})] \frac{\partial^2 v}{\partial x^2}(x, t-\bar{s}), \quad 0 < \bar{s} < \varepsilon.$$

Then with $\varepsilon \rightarrow 0$ we get $\bar{s}(\varepsilon) \rightarrow 0$ and we approximate the perturbing term with

$$\varepsilon [G(0) - G_M(0)] \frac{\partial^2 v}{\partial x^2}(x, t).$$

The approximating problem is like one perturbed by a small viscosity $\mu = \varepsilon [G(0) - G_M(0)]$.

The reader may notice that the heuristic argument just given applies to *any* two kernels which coincide for $s > \varepsilon$. The implication is that an approximation to the solution corresponding to one kernel may be obtained

*) Another type of comparison kernel is used in the Ph.D. thesis (University of Minnesota, 1983) of A. Narain for precise arguments leading to the result shown in Fig. 1.1.

by solving a problem with the other kernel, perturbed by a viscous term with a suitable selected viscosity coefficient.

In the second special case we have

$$(ii) \quad G'(0) = 0.$$

In this case, $a(x) = 1$, and

$$\frac{\partial f}{\partial t}(x, \alpha x^+) = \frac{+\alpha x}{2} \left[\frac{G''(0)}{G(0)} \right].$$

It is necessary that $G''(0) \leq 0$ if G is to be strictly monotonically decreasing in $(0, \infty)$. For the case in which $G''(0) < 0$ there will be a velocity under-shoot in the neighborhood of $t = \alpha x$ at all x .

1.3 Viscosity and transition layers

Consider the problem of a step increase of velocity for Newtonian fluids ($\mu > 0$, $\bar{\mu}(s) \equiv 0$ in (1.1)). The classical solution of this problem ((1.2, 1.3)) is given by:

$$v(x, t) = \operatorname{erfc}(x/\sqrt{4\nu t}) \quad (1.7)$$

where $\nu = \mu/\rho$ and erfc is the complementary error function.

If $\mu > 0$ is small and G has the assumed properties, it can be shown (see § 18 of [12]) that there is a transition layer around the shock solution with $\mu = 0$. This smooth transition layer exists in a small bounded domain of $\{(x, t) | x \geq 0 \text{ and } t \geq 0\}$ and its thickness scales with μ .

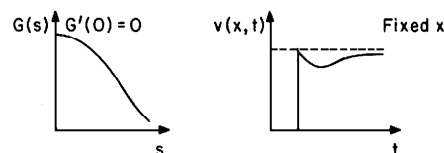


Fig. 1.2. Shock profile for the case $G'(0) = 0$

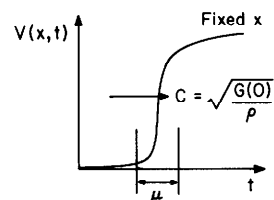


Fig. 1.3. Transition layers when $\mu > 0$ is small. Solutions with small μ can be obtained from graphs given by Tanner [18] in his analysis of the dynamics of Oldroyd fluid of the type A. The reader should compare this Fig. 1.3 with Fig. 1.1. The two cases are slightly different in that the support of the solution in Fig. 1.1 propagates. Such propagation is compatible with C^∞ smoothness but not with the analytic smoothness associated with small viscosity as in Fig. 1.3. The case $G(0)$ finite, $G'(0) = -\infty$ is intermediate between fluids of Boltzmann type and those with viscosity

2. Some formulas for the experimental determination of relaxation functions valid at large times

Many experimental measurements of relaxation functions are based on the incorrect assumption that a linear velocity profile can be achieved impulsively. This assumption is valid when the density ρ of the fluid is zero. In this case, the solution of the problem (1.2) with boundary conditions

$$v(0, t) = UH(t), \quad v(l, t) = 0$$

is a linear shear (Fig. 2.1)

$$v(x, t) = \frac{U}{l} (l - x) H(t). \tag{2.1}$$

Similar remarks apply in the problem of step increase in displacement of the boundary at $x = 0$. In this case the velocity $v(x, t) = \partial y(x, t) / \partial t$ satisfies (1.2) with $\rho = 0$ and

$$v(0, t) = Y\delta(t), \quad v(l, t) = 0.$$

The displacement field is given by a motion $\chi: (X, Y, Z) \rightarrow (X, Y + y(X, t), Z)$. It follows easily that for the step increase in displacement (Fig. 2.2)

$$y(x, t) = \frac{Y}{l} (l - x) H(t). \tag{2.2}$$

The same considerations hold in the case of sudden cessation of shear flow (Fig. 2.3). In this case we derive

$$v(x, t) = \frac{U}{l} (l - x) [1 - H(t)]. \tag{2.3}$$

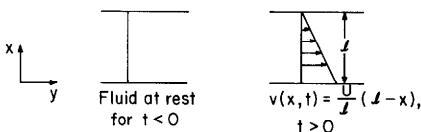


Fig. 2.1. Step increase in velocity for a fluid with density $\rho = 0$

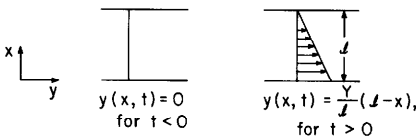


Fig. 2.2. Step increase in displacement for a fluid without inertia; $v(0, t) = Y\delta(t)$

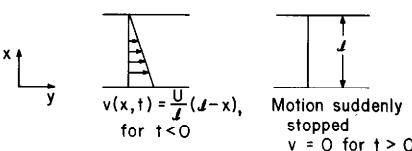


Fig. 2.3. Sudden cessation of shear in a fluid without inertia

The true solutions of these dynamical problems with impulsive data and $\rho \neq 0$ do not even resemble the solutions (2.1, 2.2, 2.3) at early times $0 < t < t^*$. The time

$$t^* = O(l/c) = O(l\sqrt{\rho/G(0)})$$

for a few reflections is such that for $t < t^*$ the right and left sides of (1.2) are both finite. If $[v, t, G, x]$ are scaled with $[U, t^*, G(0), l]$ then the left and right sides of (1.2) are dimensionless and parameter free for t^* satisfying

$$\frac{U}{l^2} [\mu + t^* G(0)] = \rho \frac{U}{t^*}. \tag{2.4}$$

For $\mu = 0$, (2.4) also gives $t^* = O(l/c)$.

For large values of $t \gg t^*$, the transients die away and the difference between the solutions (2.1, 2.2, 2.3) and the true ones tend to zero. This gives these elementary solutions status as asymptotic solutions valid for $t \gg t^*$.

The asymptotic solutions (2.1, 2.2, 2.3) are valuable for the experimental determination of the Newtonian viscosity μ and the relaxation modulus

$$\tilde{\mu}(s) = dG(s)/ds \tag{2.5}$$

for large s . These solutions should *not* be used to determine values of the relaxation modulus for small s .

The viscosity and relaxation modulus are the only material properties which appear in small amplitude expansions of the stress (see [6] and [17]). The shear stress is approximated up to terms of cubic order $O(\|\lambda_t(s)\|_h^3)$ by

$$\begin{aligned} T^{(xy)}(x, t) &\sim \mu \frac{\partial v(x, t)}{\partial x} + \int_0^\infty \tilde{\mu}(s) \lambda_t(s) ds \\ &= \mu \frac{\partial v(x, t)}{\partial x} + \int_0^\infty G(s) \frac{\partial v(x, t-s)}{\partial x} ds \end{aligned} \tag{2.6}$$

where

$$\lambda_t(s) = \frac{\partial y(x, t-s)}{\partial x} - \frac{\partial y(x, t)}{\partial x} = \int_t^{t-s} \frac{\partial v(x, \sigma)}{\partial x} d\sigma \tag{2.7}$$

The first normal-stress difference

$$N_1(x, t) = T^{(yy)} - T^{(xx)}$$

is approximated up to terms of quartic order by

$$N_1(x, t) \sim - \int_0^\infty \tilde{\mu}(s) \lambda_t^2(s) ds. \tag{2.8}$$

We may compute the large t values of the stress using these expressions and the asymptotic solutions. These expressions are for quantities which can be measured in experiments and it is therefore desirable to know when they may be used.

Clearly it is necessary that $t \gg t^*$, so that the deformation field will have very nearly attained its

asymptotic steady value. However, we must also know how the early time deformation enters into the memory of the fluid. The expression (1.1) for the shear stress may be written as

$$T^{(xy)}(x, t) = \mu \frac{\partial v(x, t)}{\partial x} + \int_0^t G(t-\tau) \frac{\partial v(x, \tau)}{\partial x} d\tau.$$

Suppose, for simplicity, that when $t > \tilde{t} \gg t^*$

$$\frac{\partial v(x, \tau)}{\partial x} \cong -\frac{U}{l}.$$

Now consider a false stress

$$\tilde{T}^{(xy)}(x, t) = \mu \frac{\partial \tilde{v}(x, t)}{\partial x} + \int_0^t G(t-\tau) \frac{\partial \tilde{v}(x, \tau)}{\partial x} d\tau$$

where

$$\frac{\partial \tilde{v}(x, \tau)}{\partial x} = -\frac{U}{l} H(\tau).$$

Then for $t > \tilde{t}$, we have

$$\begin{aligned} T^{(xy)}(x, t) - \tilde{T}^{(xy)}(x, t) &= \int_0^t G(t-\tau) \frac{\partial}{\partial x} [v(x, \tau) - \tilde{v}(x, \tau)] d\tau \\ &= \int_0^{\tilde{t}} G(t-\tau) \left[\frac{\partial v(x, \tau)}{\partial x} - \frac{\partial \tilde{v}(x, \tau)}{\partial x} \right] d\tau \\ &+ \int_{\tilde{t}}^t G(t-\tau) \left[\frac{\partial v(x, \tau)}{\partial x} - \frac{\partial \tilde{v}(x, \tau)}{\partial x} \right] d\tau. \end{aligned}$$

Therefore, if $G(t-\tilde{t})$ is small enough then, for large t ,

$$T^{(xy)}(x, t) \rightarrow \tilde{T}^{(xy)}(x, t) \quad (2.9)$$

and since $G(s) \rightarrow 0$ as $s \rightarrow \infty$, there is always a $t > t^*$ large enough so that (2.9) holds. Given \tilde{t} , the smallest $t > \tilde{t} \gg t^*$ for which (2.9) holds is given by

$$t > \tilde{t} + \lambda = O(t^* + \lambda) \quad (2.10)$$

where λ is a typical relaxation time for $G(s)$. If the stress relaxes slowly it may remember transients from early times for a long time. A material which is already in a homogeneous state of deformation may experience a stress which remembers a nonhomogeneous deformation.

Formulae giving the large time expressions for the shear stress and the first normal stress in the three problems sketched in Figs. 2.1, 2.2, 2.3 are listed below.

$$\left. \begin{aligned} T^{(xy)}(x, t) &\sim \frac{-U}{l} \left\{ \mu + \int_0^t G(s) ds \right\}, \\ N_1(x, t) &\sim \frac{-U^2}{l^2} \int_0^t s^2 G'(s) ds, \end{aligned} \right\} \begin{array}{l} \text{step increase} \\ \text{in velocity} \end{array} \quad (2.11)$$

$$\left. \begin{aligned} T^{(xy)}(x, t) &\sim \frac{-Y}{l} G(t), \\ N_1(x, t) &\sim \frac{+Y^2}{l^2} G(t), \end{aligned} \right\} \begin{array}{l} \text{step increase in} \\ \text{displacement} \end{array} \quad (2.12)$$

$$\left. \begin{aligned} T^{(xy)}(x, t) &\sim \frac{-U}{l} \int_t^\infty G(s) ds, \\ N_1(x, t) &\sim \frac{-U^2}{l^2} \int_t^\infty G'(s) (t-s)^2 ds \\ &= \frac{2U^2}{l^2} \left[\int_t^\infty s G(s) ds - t \int_t^\infty G(s) ds \right]. \end{aligned} \right\} \begin{array}{l} \text{sudden cessa-} \\ \text{tion of shear} \end{array} \quad (2.13)$$

The formulae (2.11, 2.12, 2.13) are suitable for determination of the viscosity and the relaxation function at large times ($t \gg t^* + \lambda$) from experiments with small strains. We turn now to the general linearized problem which governs these impulsive experiments.

3. Some formulae for the experimental determination of relaxation functions valid at small times

Now we are going to evaluate the shear stress and the first normal stress for the impulsive problems of Figs. 2.1, 2.2, 2.3 from the exact solutions of the linearized problem when the viscosity $\mu = 0$. The theory for this is given in [12], though other works, treating special models may be useful. Solutions for the step increase in velocity between parallel plates can be found in the book of Böhme [2] and in the papers of Denn [7] and Kazakia and Rivlin [9]. These authors consider Maxwell models with a single relaxation time. Christensen [4] has discussed this problem for Maxwell models with many relaxation times. Christensen [4] and Böhme [2] computed the shear stress at the driving wall for the step increase in velocity for a Maxwell model with a single relaxation time.

3.1 Step increase in velocity

To obtain expressions for the shear stress at the wall we consider the unsteady solution given in § 8 of [10] for the step increase in velocity (see Fig. 2.1). In that solution the moving plate is at $x = 0$ and the stationary plate is at $x = l$. For the case in which the moving plate is at $x = 0$ we ultimately have simple shear $U(1-(x/l))$

as $t \rightarrow \infty$ with shear rate $\frac{\partial v}{\partial x} \stackrel{\text{def}}{=} -\dot{\gamma}_0 = -\frac{U}{l}$. The solution of this problem is:

$$\begin{aligned} v(x, t) &= U[f(x, t) H(t-\alpha x) \\ &+ \{f(x+2l, t) H(t-\alpha(x+2l)) \\ &- f(2l-x, t) H(t-\alpha(2l-x))\} + \{\dots\} + \dots]. \end{aligned} \quad (3.1)$$

The stress at the wall $x = 0$ and $x = l$ is given by:

$$T^{(xy)}(0, t) = \int_0^t G(s) \frac{\partial v}{\partial x}(0, t-s) ds \tag{3.2}$$

and

$$T^{(xy)}(l, t) = \int_0^t G(s) \frac{\partial v}{\partial x}(l, t-s) ds. \tag{3.3}$$

If we assume an instantaneous deformation as in Fig. 2.1, then (2.6) implies that

$$T^{(xy)}(x, t) = -\frac{U}{l} \int_0^t G(s) ds, \quad x \in [0, l]. \tag{3.4}$$

However (3.1) implies that

$$\begin{aligned} \frac{\partial v}{\partial x}(0, t) = U \left\{ \frac{\partial f}{\partial x}(0, t) H(t-0) - \alpha f(0, t) \delta(t-0) \right\} \\ + 2 \left\{ \frac{\partial f}{\partial x}(2l, t) H(t-(2\alpha l)) - \alpha f(2l, t) \delta(t-(2\alpha l)) \right\} \\ + 2 \{ \dots \} + \dots \end{aligned} \tag{3.5}$$

and

$$\begin{aligned} \frac{\partial v}{\partial x}(l, t) = 2U \left[\frac{\partial f}{\partial x}(l, t) H(t-\alpha l) - \alpha f(l, t) \delta(t-\alpha l) \right] \\ + \left[\frac{\partial f}{\partial x}(3l, t) H(t-(3\alpha l)) - \alpha f(3l, t) \delta(t-(3\alpha l)) \right] \\ + \{ \dots \} + \dots \end{aligned} \tag{3.6}$$

Combining (3.5) and (3.2), we find that in the time interval $0 < t < \alpha(2l)$, the stress at the driving plate is

$$\begin{aligned} T^{(xy)}(0, t) \\ = U \int_0^t G(t-s) \frac{\partial f}{\partial x}(0, s) ds - U \alpha G(t) f(0, 0^+), \end{aligned} \tag{3.7}$$

but eq. (1.5) implies that

$$U f(0, 0^+) = v(0, 0^+) = U.$$

Hence,

$$-T^{(xy)}(0, 0^+) = U \sqrt{\rho G(0)}. \tag{3.8}$$

Combining (3.3) and (3.6) we get

$$T^{(xy)}(l, t) = 0 \quad \text{for } 0 < t < \alpha l, \tag{3.9}$$

$$-T^{(xy)}(l, \alpha l^+) = 2U \sqrt{\rho G(0)} \exp\left(\frac{\alpha l G'(0)}{2G(0)}\right). \tag{3.10}$$

In general, for $t > (2n\alpha l)$; $n = 1, 2, \dots$, we find by combining (3.5) and (3.6) with (3.2) and (3.3) that

$$\begin{aligned} -T^{(xy)}(0, t) = \left[-\int_0^t G(t-s) \frac{\partial f}{\partial x}(0, s) ds + \alpha G(t) \right] \\ + 2 \left[-\int_{(2\alpha l)}^t G(t-s) \frac{\partial f}{\partial x}(2l, s) ds \right. \\ \left. + G(t-(2\alpha l)) \exp\left(\frac{G'(0)}{2G(0)} 2\alpha l\right) \right] \\ + 2 \{ \dots \} + \dots \end{aligned} \tag{3.11}$$

and

$$\begin{aligned} -T^{(xy)}(l, t) \\ = 2U \left[\alpha G(t-\alpha l) f(l, \alpha l^+) - \int_{\alpha l}^t G(t-s) \frac{\partial f}{\partial x}(l, s) ds \right] \\ + 2U \left[\alpha G(t-(3\alpha l)) f(3l, (3\alpha l)^+) \right. \\ \left. - \int_{(3\alpha l)}^t G(t-s) \frac{\partial f}{\partial x}(3l, s) ds \right] \\ + 2 \{ \dots \} + \dots \end{aligned} \tag{3.12}$$

In order to understand (3.11) and (3.12), we need to know some features of the functions $\frac{\partial f}{\partial x}(2nl, t)$ for $n = 0, 1, 2, \dots$. For a Maxwell fluid $G(s) = K e^{-\mu s}$ and (see (7.3) of [13])

$$-\frac{\partial f}{\partial x}(x, t) = -U \sqrt{\frac{\rho \mu^2}{K}} \frac{\partial \hat{f}}{\partial \hat{x}}(\hat{x}, \hat{t}) \tag{3.13}$$

where

$$\begin{aligned} x = \sqrt{\frac{K}{\rho \mu^2}} \hat{x}, \quad t = \frac{1}{\mu} \hat{t}, \\ \frac{\partial \hat{f}}{\partial \hat{x}}(\hat{x}, \hat{t}) = -\frac{1}{2} \exp\left(-\frac{\hat{x}}{2}\right) - \frac{\hat{x}}{8} \exp\left(-\frac{\hat{x}}{2}\right) \\ + \frac{1}{2} \int_{\hat{x}}^{\hat{t}} \frac{e^{-\sigma/2}}{\sqrt{\sigma^2 - \hat{x}^2}} I_1\left(\frac{1}{2} \sqrt{\sigma^2 - \hat{x}^2}\right) d\sigma \\ + \frac{\hat{x}^2}{2} \int_{\hat{x}}^{\hat{t}} \frac{e^{-\sigma/2}}{(\sigma^2 - \hat{x}^2)} \left\{ \frac{I_1\left(\frac{1}{2} \sqrt{\sigma^2 - \hat{x}^2}\right)}{(\sigma^2 - \hat{x}^2)^{-3/2}} - \frac{1}{2} I_1\left(\frac{1}{2} \sqrt{\sigma^2 - \hat{x}^2}\right) \right\} d\sigma. \end{aligned}$$

We also recall that when a steady state

$$v(x, \infty) = \frac{U(l-x)}{l}$$

is approached we have

$$\lim_{t \rightarrow \infty} T(x, t) = -\frac{U}{l} \int_0^\infty G(s) ds, \quad x \in [0, l]. \tag{3.14}$$

There are two cases to consider:

(i) $\sqrt{G(0)\varrho} > l^{-1} \int_0^\infty G(s) ds$

and

(ii) $\sqrt{G(0)\varrho} < l^{-1} \int_0^\infty G(s) ds$.

In the first case the initial value of the stress larger than the final value (overshoot). A typical graph is sketched in Fig. 3.1(i). In the second case there is a jump of stress less than the steady state value. This case is sketched in Fig. 3.1(ii). Of course the amplitude of jumps in Fig. 3.1(i), (ii) ultimately tend to zero. Moreover in the two special cases $G'(0) = -\infty$ or $\mu > 0$ and small we will have essentially the same response as in Figs. 3.1 with smooth bumps replacing jumps. In any experiment the jumps (for $\mu = 0$) would not be vertical because step changes at the boundary are discontinuous idealizations of smooth rapid changes and if $v(0, t)$ is a continuous functions close to $UH(t-0)$, then $T^{(xy)}(0, 0^+) = 0$ but $T^{(xy)}(0, \varepsilon_1) \cong U\sqrt{G(0)\varrho}$ and

$$T^{(xy)}(l, \alpha l + \varepsilon_2) \cong 2U\sqrt{G(0)\varrho} \exp\left(\frac{\alpha l G'(0)}{2G(0)}\right)$$

for some $\varepsilon_1, \varepsilon_2 > 0$ and small. This observation follows as a consequence of the continuous dependence of the solution on the data [12] and our solution for arbitrary initial data [14].

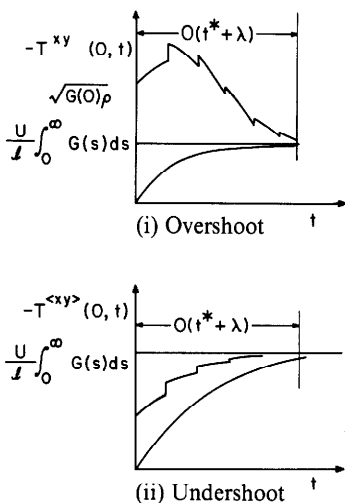


Fig. 3.1. Stress development at the lower wall for a fluid with $G(0)$ and $G'(0)$ finite and $\mu = 0$ under a step change in velocity. Graphs of this type with kernels of exponential type with one relaxation time have been computed by Böhme [2] and Christensen [4]. The smooth lines correspond to the solution (3.4)

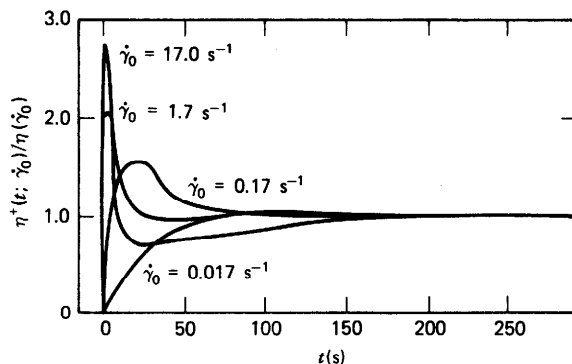


Fig. 3.2. Representations of stress development in experiments under a step change of velocity

The aforementioned results may be applied to the interpretation of experiments by Meissner [11], Huppeler et al. [8], among others. They plot

$$\frac{T^{(xy)}(0, t)}{T^{(xy)}(0, \infty)} \stackrel{\text{def}}{=} \frac{\eta^+(t)}{\eta_0}$$

where

$$T^{(xy)}(0, t) \stackrel{\text{def}}{=} -\dot{\gamma}_0 \eta^+(t) = -\frac{U}{l} \eta^+(t), \quad \eta_0 = \int_0^\infty G(s) ds.$$

Our analysis shows that at the driving plate

$$\frac{\eta^+(0^+)}{\eta_0} = \frac{l\sqrt{G(0)\varrho}}{\int_0^\infty G(s) ds}$$

where $\eta^+(\infty)/\eta_0 = 1$.

The stress response at the stationary wall is given by

$$\begin{aligned} \frac{T^{(xy)}(l, \alpha l^+)}{T^{(xy)}(l, \infty)} &= \frac{\eta^+(\alpha l^+)}{\eta_0} \\ &= \frac{2l\sqrt{\varrho G(0)}}{\int_0^\infty G(s) ds} \exp\left(\frac{\alpha l G'(0)}{2G(0)}\right) \end{aligned}$$

where $\eta^+(\infty)/\eta_0 = 1$.

Typical representations of experimental results of various authors are represented schematically in Fig. 3.2 (cf. Bird, Armstrong and Hassager, [1] Fig. A.4-9).

The experimental results represented in Fig. 3.2 do not exhibit the stress jumps, at small rates of shear, ($\dot{\gamma}_0 < 0.17 \text{ s}^{-1}$), which are required by linearized dynamics. It is possible that the conditions of the experiments were such as to make the initial jumps in stress small relative to asymptotic ($t \rightarrow \infty$) levels of stress. However, stress overshoot could possibly occur even in

the realm of linear theory. We cannot know whether or not overshoots do occur without reliable estimates of $G(0)$. The methods which are presently used to determine $G(0)$ are inadequate because they do not apply at small times.

It is perhaps also possible to explain the oscillations at small times in the stress observed by Meissner [11] in terms of larger amplitudes of stress which are generated by reflections off bounding walls for fluids of the type which support shocks or near shocks (fluids with $G(0) < \infty$, $-G'(0) \leq \infty$ with or without a small viscosity). Nonlinearity also participates in the results observed at high shears. For example, the narrowing of the width of peak region in the graphs shown in Fig. 3.2 may not be entirely explained by linear theory.

The limiting small amplitude value of the first normal stress may be computed from (2.8), which may be written as

$$N_1(x, t) \sim - \int_0^t G'(s) \left[\int_t^{t-s} \frac{\partial v(x, \sigma)}{\partial x} d\sigma \right]^2 ds$$

$$= - \int_{-\infty}^t G'(t-\tau) \left\{ \frac{\partial}{\partial x} \int_t^\tau v(x, \sigma) d\sigma \right\}^2 d\tau. \quad (3.15)$$

To compute $N_1(0, t)$ and $N_1(l, t)$ we substitute for $v(x, t)$ from (3.1). This leads to expressions for N_1 at the driving plate at $t = 0$,

$$N_1(0, 0^+) = \rho U^2 \quad (3.16)$$

and at the time of first reflection

$$N_1(l, \alpha l^+) = 4\rho U^2 \exp \left[\frac{\alpha l G'(0)}{G(0)} \right] \quad (3.17)$$

and asymptotically for $t \rightarrow \infty$, and $0 \leq x \leq l$,

$$N_1(x, \infty) = +2 \left(\frac{U}{l} \right)^2 \int_0^\infty s G(s) ds$$

$$= \left(\frac{U}{l} \right)^2 \int_0^\infty -s^2 G'(s) ds. \quad (3.18)$$

A sketch of the time development of the first normal stress $N_1(0, t)$ is given in Fig. 3.3.

3.2 Step increase in displacement

The solution of the dynamical problem for the step increase in displacement (see Fig. 2.2) is given in terms of the velocity

$$v(x, t) = Y \left\{ \frac{\partial f}{\partial t}(x, t) H(t - \alpha x) + f(x, t) \delta(t - \alpha x) \right\}$$

$$- \left\{ \frac{\partial f}{\partial t}(2l - x, t) H(t - \alpha(2l - x)) + f(2l - x, t) \delta(t - \alpha(2l - x)) \right\} + \{ \dots \} - \dots \quad (3.19)$$

We recall that the shear stress is given by:

$$T^{(xy)}(x, t) = \int_0^\infty G'(s) \lambda'(s) ds$$

$$= \int_{-\infty}^t G'(t-\tau) \left\{ \frac{\partial}{\partial x} \int_t^\tau v(x, \sigma) d\sigma \right\} d\tau \quad (3.20)$$

and the first normal stress is given by

$$N_1(x, t) = - \int_0^\infty G'(s) (\lambda'(s))^2 ds$$

$$= - \int_{-\infty}^t G'(t-\tau) \left\{ \frac{\partial}{\partial x} \int_t^\tau v(x, \sigma) d\sigma \right\}^2 d\tau \quad (3.21)$$

where

$$\lambda'(s) \stackrel{\text{def}}{=} \int_t^{t-s} \frac{\partial v}{\partial x}(x, \sigma) d\sigma.$$

Now we substitute (3.19) in (3.20) and (3.21) to evaluate the result for $\alpha x < t < \alpha(2l - x)$. Taking the limit for $x = 0$ and $t \rightarrow 0$ we find that

$$-T^{(xy)}(0, 0^+) = \frac{Y}{2} \sqrt{\frac{\rho}{G(0)}} (-G'(0)) \quad (3.22)$$

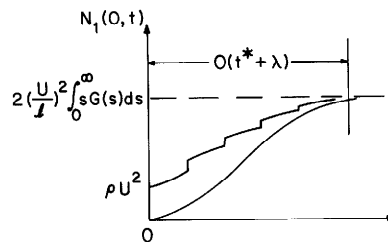


Fig. 3.3. Sketch of development of the first normal stress at the wall $x = 0$ when $\rho U^2 < 2 \left(\frac{U}{l} \right)^2 \int_0^\infty s G(s) ds$

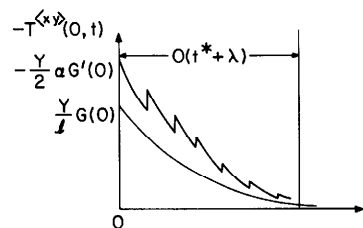


Fig. 3.4. Sketch of development of shear stress for sudden displacement when $-\frac{Y}{2} \frac{\alpha G'(0)}{2} > \frac{Y}{l} G(0)$

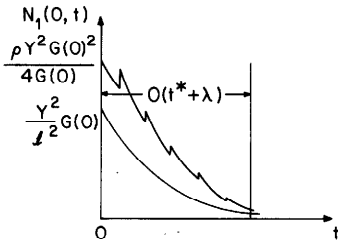


Fig. 3.5. Sketch of the first normal-stress difference at the wall $x = 0$ for shearing displacement when $\frac{\rho Y^2 G'(0)^2}{4G(0)^2} > \frac{Y^2}{l^2} G(0)$

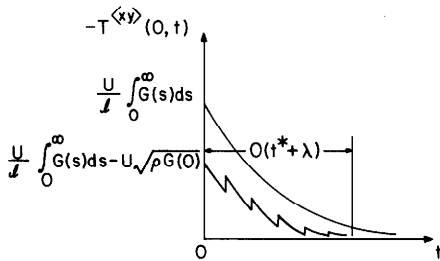


Fig. 3.6. Sketch of shear stress at $x = 0$ when $\frac{U}{l} \int_0^\infty G(s) ds - U\sqrt{\rho G(0)} > 0$ in sudden cessation of flow

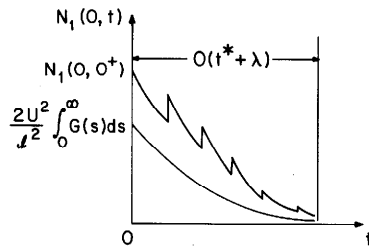


Fig. 3.7. Sketch of First normal-stress difference at $x = 0$ when $N_1(0, 0^+) > \frac{2U^2}{l^2} \int_0^\infty G(s) ds$ in sudden cessation of flow

and

$$N_1(0, 0^+) = \frac{\rho Y^2 G'(0)^2}{4G(0)^2}. \tag{3.23}$$

To compute the shear stress and the first normal-stress difference on the stationary wall at $x = l$ at the time of first reflection let $t \rightarrow \alpha l^+$. This gives:

$$T^{(xy)}(l, \alpha l^+) = Y \left[\alpha G'(0) \exp\left(\frac{\alpha l G'(0)}{2G(0)}\right) - 2\alpha G(0) \frac{\partial f}{\partial t}(l, \alpha l^+) \right] \tag{3.24}$$

and

$$N_1(l, \alpha l^+) = 4\rho Y^2 \exp\left(\frac{\alpha l G'(0)}{G(0)}\right) \left[\alpha l \left\{ \frac{3}{8} \left(\frac{G'(0)}{G(0)}\right)^2 - \frac{G''(0)}{2G(0)} \right\} + \frac{G'(0)}{2G(0)} \right]^2. \tag{3.25}$$

3.3 Sudden cessation of flow

The dynamical problem for sudden cessation of flow (see Fig. 2.3) is given by:

$$\rho \frac{\partial v}{\partial t} = \int_0^l G(s) \frac{\partial^2 v}{\partial x^2}(x, t-s) ds,$$

$$v(x, t) = \frac{U}{l}(l-x) \quad \forall t < 0, \tag{3.26}$$

$$v(0, t) = U[1 - H(t-0)],$$

$v(x, t)$ is bounded.

It is easy to see that the solution of (3.26) is:

$$v(x, t) = \frac{U}{l}(l-x) - \tilde{v}(x, t) \tag{3.27}$$

where $\tilde{v}(x, t)$ is the same as $v(x, t)$ in (3.1). Now substituting (3.27) in (3.20) and (3.21) we get:

$$-T^{(xy)}(0, 0^+) = + \frac{U}{l} \int_0^\infty G(s) ds - U\sqrt{\rho G(0)}, \tag{3.28}$$

$$N_1(0, 0^+) = \frac{2U^2}{l^2} \int_0^\infty s G(s) ds + \rho U^2 - \frac{2U^2 \alpha}{l} \int_0^\infty G(s) ds$$

and

$$-T^{(xy)}(l, \alpha l^+) \tag{3.29}$$

$$= \frac{U}{l} \int_0^\infty G(s) ds - 2U\sqrt{\rho G(0)} \exp\left(\frac{\alpha l G'(0)}{2G(0)}\right),$$

$$N_1(l, \alpha l^+) = \frac{2U^2}{l^2} \int_0^\infty s G(s) ds + 4\rho U^2 \exp\left(\frac{\alpha l G'(0)}{G(0)}\right)$$

$$- \frac{4U^2 \alpha}{l} \exp\left(\frac{\alpha l G'(0)}{2G(0)}\right) \int_0^\infty G(s) ds.$$

4. Summary

Exact formulae for the shear stress and the first normal stress in the linearized approximation are given in § 3. These formulas apply at every instant $t > 0$ and every place x , $0 \leq x \leq l$. The major interest in these formulae are at the driving plate at $x = 0$ which is in motion and at the stationary plate at $x = l$ where the

stresses are measured. In fact, the experiments are nearly always conducted with cone and plate rheometers, and the relation between parallel plate theories and the cone and plate data should be made more precise. Presumably one uses average l in the cone and plate where the recording instruments are mounted. The formulas in § 3 are complicated. In this summary we shall list the values of the stress at the driving plate at the instant $t = 0^+$ after the motion is started and at the recording plate at $x = l$ at the instant $t = \alpha l^+$ ($\alpha = l/c$, $c = \sqrt{G(0)/\rho}$) after first reflection. For completeness we also repeat the asymptotic formulas for $t > \tilde{t} + \lambda$ which are given in § 2. We have not computed the stresses for impulsive motions in fluids with viscosity $\mu \neq 0$. All the formulas appearing below have $\mu = 0$. We have already mentioned that there is continuity of the solution with $\mu \rightarrow 0$, so that the formulas we give are good approximations to the formulas when μ is small.

(i) Step increase in velocity:

$$\begin{aligned}
 -T^{(xy)}(0, 0^+) &= U\sqrt{\rho G(0)}, \\
 -T^{(xy)}(l, \alpha l^+) &= 2U\sqrt{\rho G(0)} \exp[\alpha l G'(0)/2G(0)], \\
 -T^{(xy)}(x, t) &\sim \frac{U}{l} \int_0^t G(s) ds, \quad t > \tilde{t} + \lambda, \\
 N_1(0, 0^+) &= \rho U^2, \\
 N_1(l, \alpha l^+) &= 4\rho U^2 \exp\left[\frac{\alpha l G'(0)}{G(0)}\right], \\
 N_1(x, t) &\sim 2 \frac{U^2}{l^2} \int_0^t s G(s) ds, \quad t > \tilde{t} + \lambda.
 \end{aligned}$$

(ii) Step increase in displacement:

$$\begin{aligned}
 -T^{(xy)}(0, 0^+) &= -\frac{Y}{2} G'(0) \sqrt{\frac{\rho}{G(0)}}, \\
 -T^{(xy)}(l, \alpha l^+) &= -Y \left[\alpha G'(0) \exp\left(\frac{\alpha l G'(0)}{2G(0)}\right) \right. \\
 &\quad \left. - 2\alpha G(0) \frac{\partial f}{\partial t}(l, \alpha l^+) \right],
 \end{aligned}$$

where $\partial f(l, \alpha l^+)/\partial t$ is given by (1.5)₂,

$$\begin{aligned}
 -T^{(xy)}(x, t) &\sim \frac{Y}{l} G(t), \quad t > \tilde{t} + \lambda, \\
 N_1(0, 0^+) &= \frac{\rho Y^2 G'(0)^2}{4G(0)^2},
 \end{aligned}$$

$$\begin{aligned}
 N_1(l, \alpha l^+) &= 4\rho U^2 \exp\left(\frac{\alpha l G'(0)}{G(0)}\right) \\
 &\quad \cdot \left[\alpha l \left\{ \frac{3}{8} \frac{G'(0)^2}{G(0)^2} - \frac{G''(0)}{2G(0)} \right\} + \frac{G'(0)}{2G(0)} \right]^2, \\
 N_1(x, t) &\sim \frac{Y^2}{l^2} G(t), \quad t > \tilde{t} + \lambda.
 \end{aligned}$$

(iii) Sudden cessation of flow:

$$\begin{aligned}
 -T^{(xy)}(0, 0^+) &= \frac{U}{l} \int_0^\infty G(s) ds - U\sqrt{\rho G(0)}, \\
 -T^{(xy)}(l, \alpha l^+) &= \frac{U}{l} \int_0^\infty G(s) ds - 2U\sqrt{\rho G(0)} \exp\left[\frac{\alpha l G'(0)}{2G(0)}\right], \\
 -T^{(xy)}(x, t) &\sim \frac{U}{l} \int_t^\infty G(s) ds, \quad t > \tilde{t} + \lambda, \\
 N_1(0, 0^+) &= \frac{2U^2}{l^2} \int_0^\infty s G(s) ds + \rho U^2 - \frac{2U^2 \alpha}{l} \int_0^\infty G(s) ds, \\
 N_1(l, \alpha l^+) &= \frac{2U^2}{l^2} \int_0^\infty s G(s) ds + 4\rho U^2 \exp\left(\frac{\alpha l G'(0)}{G(0)}\right) \\
 &\quad - \frac{4U^2 \alpha}{l} \exp\left(\frac{\alpha l G'(0)}{2G(0)}\right) \int_0^\infty G(s) ds, \\
 N_1(x, t) &\sim \frac{2U^2}{l^2} \left[\int_t^\infty s G(s) ds - t \int_t^\infty G(s) ds \right], \\
 &\quad t > \tilde{t} + \lambda.
 \end{aligned}$$

Acknowledgement

The results in this paper are taken from the Ph.D. Thesis of A. Narain. The research was supported by the U.S. Army.

References

1. Bird, R. B., R. C. Armstrong, O. Hassager, Dynamics of Polymeric Liquids, Vol. I, John Wiley (New York 1977).
2. Böhme, G., Strömungsmechanik Nicht-Newtonscher Fluide, B. G. Teubner (Stuttgart 1981).
3. Buchen, P. W., Mainardi, J. de Mécanique **14**, 597-608 (1975).
4. Christensen, R. N., Theory of Viscoelasticity - An Introduction, Academic Press (New York and London 1971).
5. Coleman, B. D., M. E. Gurtin, Arch. Rational Mech. Anal. **19**, 239-265 (1965).
6. Coleman, B. D., H. Markovitz, J. Polym. Sci. **12**, 2195-2207 (1974).
7. Denn, M. M., K. C. Porteous, Chem. Engng. J. (2), 280-286 (1971).

8. Huppler, J. D., I. F. MacDonald, E. Ashare, T. W. Spriggs, R. B. Bird, L. A. Holmes, *Trans Soc. Rheology* **11**, 181–204 (1967).
9. Kazakia, J. Y., R. S. Rivlin, *Rheol. Acta* **20**, 111–127 (1981).
10. Kee, D. D., P. J. Carreau, *J. Non-Newtonian Fluid Mech.* **6**, 127–143 (1979).
11. Meissner, J., *J. Appl. Polym. Sci.* **16**, 2877–2899 (1972).
12. Narain, A., D. D. Joseph, *Rheol. Acta* **21**, 228–250 (1982).
13. Narain, A., D. D. Joseph: Classification of Linear Viscoelastic Solids Based on a Failure Criterion. To appear in *J. Elasticity* (1984).
14. Narain, A., D. D. Joseph: Linearized Dynamics of Shearing Motion Perturbing the State of Rest of Simple Materials. To appear in *Conference on Differential Equations, Equadiff, Wurgburg* (1983).
15. Renardy, M., *Rheol. Acta* **21**, 251–254 (1982).
16. Renardy, M.: On the Domain Space for Constructive Laws in Linear Viscoelasticity (to appear).
17. Saut, J. C., D. D. Joseph, *Arch. Rational Mech. Anal.* **81**, 53–95 (1983).
18. Tanner, R. I., *ZAMP* **13**, 573 (1962).

(Received December 15, 1982;
in revised form April 22, 1983)

Authors' addresses:

Prof. A. Narain
Department of Mechanical Engineering
and Engineering Mechanics
Michigan Technological University
Houghton, MI 49931 (USA)

Prof. D. D. Joseph
Department of Aerospace Engineering
and Mechanics, University of Minnesota
107 Akerman Hall
110 Union Street S.E.
Minneapolis, MN 55455 (USA)

Note added in proof: The dynamics of the flow for a four constant Oldroyd model was also considered by K. Strauß (*Rheol. Acta* **16**, 385–393 (1977)).